

# A MODEL OF DYNAMIC QUENCHING OF FLUORESCENCE IN GLOBULAR PROTEINS

ENRICO GRATTON, DAVID M. JAMESON, AND GREGORIO WEBER

*Departments of Physics and Biochemistry, University of Illinois at Urbana-Champaign, Urbana, Illinois 61801*

BERNARD ALPERT

*Laboratoire de Biologie Physico-Chimique, Universite de Paris VII, 75251 Paris*

**ABSTRACT** A model is presented for the quenching of a fluorophore in a protein interior. At low quencher concentration the quenching process is determined by the acquisition rate of quencher by the protein, the migration rate of quencher in the protein interior, and the exit rate of quencher from the protein. In cases where the fluorescence emission observed in the absence of quencher could be described by a single exponential decay, the presence of quencher led to doubly exponential decay times, and the aforementioned exit rates of the quencher could be determined from experimental data. At high quencher concentration, the processes became more complex, and the deterministic rate equations used at low quencher concentration had to be modified to take into account the Poisson distribution of quencher molecules throughout the protein ensemble and also by using a migration rate for quencher in the protein interior that is a function of the quencher concentration. Simulations performed for typical fluorescent probes in proteins showed good agreement with experiments.

## INTRODUCTION

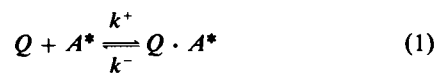
Molecular oxygen is known to be an efficient quencher of the fluorescence of aromatic molecules (1). Oxygen quenching of tryptophan fluorescence in a number of globular proteins has been studied by Lakowicz and Weber (2). In these experiments, no tryptophan residue seemed to be excluded from quenching, suggesting that rapid oxygen diffusion occurs in all regions of the protein. Most importantly, the dynamic character of the quenching process was demonstrated by the parallel decrease of the fluorescence intensity and lifetime. In the present paper, we present a general model for the quenching process that encompasses these observations, as well as some others apparently contradicting this latter finding (3).

We limit ourselves to the consideration of short-range interaction of excited fluorophore and quencher, whether this process involves the time of a collision or that of a longer-lived complex. We exclude such processes as nonradiative energy transfer with a radius of action greater than the van der Waals interaction radius, i.e., our treatment was restricted to "colorless" quenchers. In addition, we consider only the case of unity quenching. In the second section we review one model for the quenching of small molecules in solution. In the third section we extend the model to globular proteins. In the last section, we show that

the proposed model explains an apparent contradiction between the quenching by molecular oxygen of the intrinsic tryptophan fluorescence of proteins (2) and the quenching of the fluorescence of pyrenebutyric acid protein adducts (3).

## DERIVATION OF THE BASIC EQUATIONS FOR DYNAMIC QUENCHING

In the following we assume that the quenching process requires a transient excited state complex between the quencher and the fluorescent molecule (4). Consider the following reaction:



where  $Q$  is a quencher molecule and  $A^*$  a fluorescent molecule.  $k^+[Q]$  is the pseudo-first order rate for formation of the complex, and  $k^-$  is its dissociation rate. The fluorescent probe has a characteristic single exponential radiative decay rate  $\Gamma$ . The complex  $Q \cdot A^*$  has, in addition to  $\Gamma$ , a nonradiative quenching rate or intrinsic quenching constant  $\chi$  (5). In Fig. 1 we represent schematically the diagram for the excited-state reaction, where  $x = [A^*]$  and  $y = [Q \cdot A^*]$ .

The equilibrium concentration of species  $x$  and  $y$  is given by

$$k^+[Q] x = k^- y. \quad (2)$$

Dr. Jameson's present address is the Department of Pharmacology, University of Texas Health Science Center at Dallas, Dallas, TX 75235

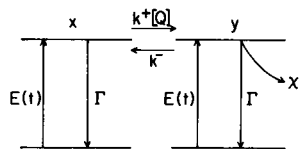


FIGURE 1 Diagram of the quenching process in solution.  $E(t)$  is the pumping function,  $\Gamma$  the radiative decay rate,  $k^+[Q]$  the rate of association,  $k^-$  the rate of dissociation, and  $\chi$  the nonradiative decay rate due to the quenching process.  $x$  and  $y$  represent concentration of free and associated fluorophores, respectively.

The differential equations describing the scheme presented in Fig. 1 after a pulse excitation are

$$\begin{aligned}\frac{dx}{dt} &= -\Gamma_0 x + yk^- \\ \frac{dy}{dt} &= k^+[Q]x - \Gamma_1 y\end{aligned}\quad (3)$$

where

$$\begin{aligned}\Gamma_0 &= \Gamma + k^+[Q] \\ \Gamma_1 &= \Gamma + \chi + k^-.\end{aligned}\quad (4)$$

The solution of this system is

$$\begin{aligned}x(t) &= \alpha_{0x}e^{-m_0t} + \alpha_{1x}e^{-m_1t} \\ y(t) &= \alpha_{0y}e^{-m_0t} + \alpha_{1y}e^{-m_1t}\end{aligned}\quad (5)$$

where

$$\begin{aligned}m_{0,1} &= \frac{(\Gamma_0 + \Gamma_1) \pm \sqrt{(\Gamma_0 - \Gamma_1)^2 + 4k^-k^+[Q]}}{2} \\ \alpha_{0x} &= \frac{x_0(\Gamma_0 - m_1) - k^-y_0}{m_0 - m_1}; \quad \alpha_{1x} = \frac{k^-y_0 - x_0(\Gamma_0 - m_0)}{m_0 - m_1} \\ \alpha_{0y} &= \frac{y_0(\Gamma_1 - m_1) - k^+[Q]x_0}{m_0 - m_1}; \\ \alpha_{1y} &= \frac{k^+[Q]x_0 - y_0(\Gamma_1 - m_0)}{m_0 - m_1}.\end{aligned}\quad (6)$$

In the above expressions  $x_0$  and  $y_0$  are the concentration of the excited species  $x$  and  $y$ , respectively, immediately after the excitation. When species  $x$  and  $y$  have the same absorption coefficient, or if excitation is at an isosbestic point, and when these species have the same emission spectrum, then  $x_0$  and  $y_0$  are proportional to  $x$  and  $y$ . Also, the relation  $y_0/x_0 = k^+[Q]/k^-$  holds.  $x(t)$  and  $y(t)$  are proportional to the time decay of the fluorescence. The time behavior of the fluorescence emission  $F(t)$  is described by two exponential components with characteristic rates  $m_0$  and  $m_1$

$$\begin{aligned}F_0(t) &= (\alpha_{0x} + \alpha_{0y})e^{-m_0t}; \quad F_1(t) = (\alpha_{1x} + \alpha_{1y})e^{-m_1t} \\ F(t) &= F_0(t) + F_1(t),\end{aligned}\quad (7)$$

where  $F_0(t)$  and  $F_1(t)$  are proportional to the fluorescence

emission of the component with decay rate  $m_0$  and  $m_1$ , respectively. The steady state fluorescence emission  $\langle F \rangle$  is given by

$$\langle F \rangle = \frac{(\alpha_{0x} + \alpha_{0y})}{m_0} + \frac{(\alpha_{1x} + \alpha_{1y})}{m_1}.\quad (8)$$

To better understand the meaning of the derived equations we may analyze the order of magnitude of the various rate constants. Generally, one assumes that the quenching rate  $\chi$  is large compared with  $\Gamma$  and  $k^-$  for low quencher concentration (6).  $\chi$  is probably on the order of  $10^{12} \text{ s}^{-1}$ , while the intrinsic fluorescence decay rate  $\Gamma$  is on the order of  $10^8$  to  $10^9 \text{ s}^{-1}$ . An ultimate limit to the value of  $k^+$  and  $k^-$  is imposed by the diffusional rate of the quencher. The typical diffusional rate value in fluid solvents at room temperature is on the order of  $10^{10} \text{ s}^{-1} \text{ mol}^{-1}$  (7). At high quencher concentration, deviation from this pure diffusional model can also be observed (8–10).

If  $\chi \gg k^-$  then quenching is “strong quenching” (3), that is, there is no appreciable contribution to the emission from dissociating complexes and the expressions for  $m_0$ ,  $m_1$ , and the preexponential factors are simplified

$$\begin{aligned}m_0 &\approx \Gamma_0 = \Gamma + k^+[Q] \\ m_1 &\approx \Gamma_1 = \Gamma + \chi + k^- \approx \chi\end{aligned}\quad (9)$$

$$\begin{aligned}\alpha_{0x} &= x_0 + \frac{k^-y_0}{\Gamma_1}; \quad \alpha_{1x} = -\frac{k^-y_0}{\Gamma_1} \\ \alpha_{0y} &= \frac{k^+[Q]x_0}{\Gamma_1}; \quad \alpha_{1y} = -\frac{k^+[Q]x_0}{\Gamma_1} + y_0\end{aligned}$$

$$\begin{aligned}\langle F \rangle &= \frac{1}{\Gamma_0} \left( x_0 + \frac{k^-y_0}{\Gamma_1} + \frac{k^+[Q]x_0}{\Gamma_1} \right) \\ &\quad + \frac{1}{\Gamma_1} \left( -\frac{k^-y_0}{\Gamma_1} - \frac{k^+[Q]x_0}{\Gamma_1} + y_0 \right).\end{aligned}$$

Note that even in the absence of formation of a stable complex a positive curvature can appear in a Stern-Volmer plot when  $\Gamma_0$  becomes comparable to  $\Gamma_1$ .

The time behavior of the fluorescence is described by two exponential decaying components (Eq. 7). If  $\Gamma_1$  is large, only  $\alpha_{0x}$  has a nonvanishing value. The decay rate of this term is  $\Gamma_0 = \Gamma + k^+[Q]$ . The steady state fluorescence intensity is  $\langle F \rangle = x_0/\Gamma_0$ . Usually, in a quenching experiment, the intensity and the lifetime of the fluorescence are measured as a function of the quencher concentration. A plot of  $\Gamma_0$  vs. quencher concentration (Stern-Volmer plot) is linear with an intercept of  $\Gamma$ , the unquenched decay rate, and a slope of  $k^+$ , the bimolecular quenching constant. The quenching rate  $\chi$  is too large to be measured directly by existing techniques. A plot of  $1/\langle F \rangle$  vs. quencher concentration is also linear and has the same slope  $k^+$ . The value of  $k^+$  has been determined for oxygen in water for different fluorescent molecules (7, 11). The value generally found ( $k^+ \approx 1.2 \cdot 10^{10} \text{ M}^{-1} \text{ s}^{-1}$ ) at 20°C corresponds to the

diffusion limit for the encounter rate between quencher and fluorophore. Thus, for oxygen at low concentration, no activation barrier for the formation of the quenchable complex seems to exist, and the efficiency of quenching is limited only by the rate of collision. When the collision rate is not limiting, there is a barrier (energetic or entropic) to the quenching process. We still have  $\langle F \rangle = x_0/\Gamma_0$  but with  $x_0 = 1/(1 + k^+[Q]/k^-)$ .

The derivation of the quenching expressions for a small molecule in solution demonstrates that dynamic quenching is generally described by a simple scheme whatever the efficiency of the quenching process. However, we can anticipate that if  $\chi$  is not very large compared with  $\Gamma$  and  $k^-$ , a complex process will result. In this case, a double exponential decay of the fluorescence emission can be measured giving separate information on the rates  $k^+$ ,  $\chi$ , and  $k^-$ . We show in the following section that this case arises in the quenching of a fluorophore in the interior of a protein.

#### QUENCHING EQUATIONS FOR A FLUORESCENCE PROBE INSIDE A PROTEIN

The same approach used for the quenching process in solution can be used for quenching in proteins. However, the physical meaning of the parameters of the model is quite different. In the following, we assume that the probe is in the protein interior isolated from the solvent. This restrictive assumption is valid in a limited number of cases, one of which is described in the following companion paper. Following this assumption the quencher must penetrate the protein before actual quenching takes place. Penetration proceeds with rate  $k^+[Q]$ , a term formally identical to that describing the formation of the complex in the previous derivation of the quenching equations in solution (Fig. 2). In the present case,  $k^+$  depends in the first approximation on the energetic or entropic barrier for oxygen entry to the protein. Once inside the protein, the quencher can migrate in the protein matrix and reach the fluorescent probe at a rate  $\chi$ . Although the protein is hardly a homogeneous medium we assume a unique value of  $\chi$  that represents an average migration inside the protein. This term is equivalent to the rate of quenching

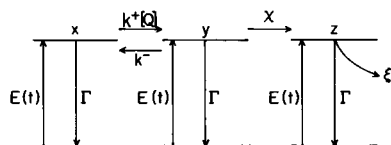


FIGURE 2 Diagram of the quenching process for a probe inside a protein.  $E(t)$  is the pumping function,  $\Gamma$  the radiative decay rate,  $k^+[Q]$  the rate of penetration of the quencher into the protein,  $k^-$  the exit rate,  $\chi$  the rate of migration, and  $\xi$  the rate of quenching.  $x$ ,  $y$ , and  $z$  represent concentration of protein macromolecules without a quencher, with some quencher, and with a quencher interacting with the fluorophore respectively at the time of excitation.

after the formation of the complex that we already introduced in the previous section. We indicate the effective quenching rate with  $\xi$  (see Fig. 2). We assume, as we did in the solution case, that  $\xi$  is large compared with  $k^-$ ,  $\Gamma$ , and  $\chi$ . The efficiency of the quenching process is then taken as unity, i.e., the back reaction rate  $\chi_-$  is negligible.

The differential equations describing this scheme are

$$\begin{aligned}\frac{dx}{dt} &= -\Gamma_0 x + k^- y \\ \frac{dy}{dt} &= +k^+[Q] x - \Gamma_1 y \\ \frac{dz}{dt} &= \chi y - \Gamma_2 z\end{aligned}\quad (10)$$

where

$$\begin{aligned}\Gamma_0 &= \Gamma + k^+[Q] \\ \Gamma_1 &= \Gamma + \chi + k^- \\ \Gamma_2 &= \Gamma + \xi\end{aligned}\quad (11)$$

$x$  represents the concentration of excited fluorophores in proteins not containing quencher molecules,  $y$  is the concentration of excited fluorophores in proteins containing quencher molecules, and  $z$  is the concentration of fluorophores associated with the quencher.

The first two equations are independent of  $z$ . The solution for  $x$  and  $y$  is identical to the one already obtained in the previous section but the parameters have a different meaning. The solution for  $z$  is

$$\begin{aligned}z(t) &= \frac{k^+[Q] \alpha_{0y} e^{-m_0 t}}{\Gamma_2 - m_0} + \frac{k^+[Q] \alpha_{1y} e^{-m_1 t}}{\Gamma_2 - m_1} \\ &+ \left( z_0 - \frac{k^+[Q] \alpha_{0y}}{\Gamma_2 - m_0} - \frac{k^+[Q] \alpha_{1y}}{\Gamma_2 - m_1} \right) e^{-\Gamma_2 t}.\end{aligned}\quad (12)$$

If  $\Gamma_2$  is large and  $z_0 = 0$ , then the contribution of  $z$  is negligible because of the vanishing value of the preexponential factor. According to this hypothesis, the fluorescence should decay with two exponential components having rates  $m_0$  and  $m_1$ . The values of  $m_0$  and  $m_1$  depend on the rates  $k^+[Q]$ ,  $k^-$ ,  $\Gamma$ , and  $\chi$ . These rates are independent of the initial population  $x_0$  and  $y_0$  of species  $x$  and  $y$ , as are  $m_0$  and  $m_1$ .

As the concentration of the quencher increases, the number of quenchers per molecule of protein will also increase and follow a discrete Poisson distribution. The probability of having  $r$  molecules of quencher per protein would be

$$p(r) = \frac{e^{-n} n^r}{r!} \quad r = 0, 1, 2, \dots \quad (13)$$

where  $n$  is the average number of quencher molecules inside the protein. The value of  $n$  depends on  $k^+$  and  $k^-$

$$n = \frac{k^+[Q]}{k^-}.\quad (14)$$

The value of  $\chi$  also depends on the quencher concentration. For quencher molecules already inside the protein at excitation, the times to reach the fluorophore will depend on their proximity to it. This effect is similar to the high concentration diffusion limit usually considered for fluorescence quenching (8–10).

In order to analyze experimental data following such a complex model, we consider some limiting situations:

(a) At low quencher concentration ( $n \ll 1$ ) the fraction of proteins with molecules of oxygen already inside the matrix at the time of excitation may be neglected. A double exponential decay of the fluorescence describes the quenching process.

At low quencher concentration the rate  $k^+[Q]$  is small compared with  $\Gamma$  and  $\chi$ . The experimentally measurable values of  $m_0$  and  $m_1$  are given by

$$\begin{aligned} m_0 &= \Gamma_0 = \Gamma + k^+[Q] \\ m_1 &= \Gamma_1 = \Gamma + \chi + k^- \end{aligned} \quad (15)$$

These expressions are identical to those found in the previous section. However, here the condition is that  $k^+[Q]$  should be small instead of  $\chi$  being large. The initial slope of the plot of  $m_0$  vs.  $[Q]$  gives  $k^+$ .

The plot of  $m_1$  vs.  $[Q]$  gives the value of  $\Gamma + \chi + k^-$  directly. To determine  $\chi$  and  $k^-$  independently, an additional quantity is needed: the fraction  $f_1$  of molecules decaying with rate  $m_1$ . The initial slope of the plot of  $f_1$  vs.  $[Q]$  is given by

$$\left( \frac{df_1}{d[Q]} \right)_{[Q]=0} = \frac{k^+\Gamma}{k^-\Gamma_1} \quad (16)$$

The values of  $k^+$ ,  $\Gamma$  and  $\Gamma_1$  already being known, this expression gives  $k^-$ . This analysis shows that, in the low quencher concentration limit, the rates describing the quenching process can be individually determined.

(b) At sufficiently high quencher concentration ( $n > 1$ ) the distribution of quencher among proteins is the most important determinant of the quenching and fixes the quenching rate  $\chi$ . A protein with no quencher at the time of excitation will be quenched at a rate  $\chi$  while a protein with one or more quenchers inside at the time of excitation will be quenched at a higher rate  $\chi'$ . The difference between  $\chi$  and  $\chi'$  may be rationalized if we consider that the quencher already inside the protein at the time of excitation is in better position to reach the buried fluorophore, in comparison with the quencher outside the protein. The solution of the general case for high quencher concentration is quite complex. We choose to follow a semiempirical approach. We simplify the Poisson distribution by considering only proteins without a quencher [fraction =  $p(0)$ ] and proteins with quenchers at the time of excitation [fraction =  $1 - p(0)$ ]. The solution of the differential equation for the fraction of proteins with no quencher is the same as that found in the previous paragraph. For the protein molecules with quenchers, we assume that the quenching process is

fast enough for the rate  $k^+[Q]$  to be neglected. Thus, the proteins with quenchers can be treated as an independent species. The total fluorescence is then the sum over two species with different fractional weights

$$F(t) = p(0) F_0(t) + [1 - p(0)] F_1(t) \quad (17)$$

where  $F_0(t)$  has already been derived above and

$$F_1(t) = \exp(-m_2 t) \quad (18)$$

where  $m_2 = \Gamma + \chi' + k^-$ . If  $\chi' \gg \Gamma$ , the situation approaches that of quenching by a ground-state complex.

(c) The possibility of having a quencher in a cavity inside the protein close to the fluorophore is not excluded. This particular species will have a large quenching rate ( $\chi' \gg \Gamma$ ) and makes a negligible contribution to the "dynamic quenching" as detected by lifetime measurements. In such a case, only the intensity of the fluorescence would be affected. This species corresponds in the limit to the formation of a ground-state complex of fluorophore and quencher.

## REPRESENTATION AND DISCUSSION OF THE MODELS OF PROTEIN QUENCHING

We report the results of a calculation of the fluorescent intensities and apparent lifetimes according to the proposed model. Simulations were performed for three different fluorophores having different unquenched fluorescence decay rates. We recall that these simulations of the quenching process are of exclusive dynamic character. These three fluorophores were chosen because oxygen quenching data of protein adducts of these probes are available in the literature (2, 3, 12). The decay rates of the probes were  $3.3 \times 10^8 \text{ s}^{-1}$ , for a tryptophan emission,  $5 \times 10^7 \text{ s}^{-1}$ , which corresponds to metal-free porphyrin emission, and  $5 \times 10^6 \text{ s}^{-1}$ , which corresponds to pyrene emission.

For the long-lived fluorescence from pyrenebutyrate-bovine serum albumin adducts, linear Stern-Volmer plots were observed for both lifetime and intensity data at low oxygen concentration with an apparent very low Stern-Volmer constant (3). For the quenching of protein tryptophan, linear plots were also observed for both intensity and lifetime with a relatively large Stern-Volmer constant (2). In contrast, for porphyrin protein adducts, highly curved plots are reported for the intensity, and an almost linear plot for the lifetime (12); the apparent Stern-Volmer constant has an intermediate value. In our simulations we use a value of  $5 \times 10^8 \text{ M}^{-1} \text{ s}^{-1}$  for  $k^+$ , which is well below the diffusion-controlled rate. This value is justified by the experimental results reported in the following companion paper. Vaughan and Weber (3) found a value in this range for  $k^+$  for the quenching of a pyrenebutyrate-bovine serum albumin adduct. For  $k^-$ , the exit rate, we choose  $2 \times 10^7 \text{ s}^{-1}$  to have a reasonable magnitude for the partition coefficient of oxygen inside the protein. A possible value

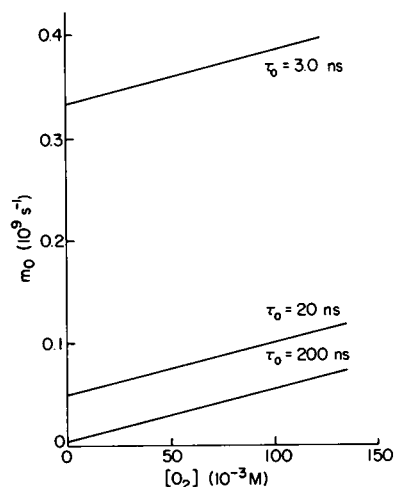


FIGURE 3 Values of  $m_0$  as a function of oxygen concentration for three probes having different lifetimes.

for  $\chi$  can be  $3 \times 10^8 \text{ s}^{-1}$ , as we discuss later on. In Fig. 3 we report the values of  $m_0$  as a function of the quencher concentration using Eqs. 5–8, valid in the low concentration limit for the three probes. The slopes of the three lines in Fig. 3 are equal because the same value of  $k^+$ , independent of the fluorescence decay rate, is assumed. The intercept is the decay rate in the absence of the quencher. As shown in Fig. 3 the ratios of the value of  $m_0$  at 0.1 M quencher concentration with respect to the unquenched value are 1.15, 2, and 8.5 for tryptophan, porphyrin, and pyrene adducts, respectively. For the case of tryptophan, this small relative change (15% in  $m_0$ ) is very difficult to observe under normal experimental conditions. The value of  $m_1$ , which is independent of the quencher concentration in the low concentration limit (Eq. 13), is  $6.5 \times 10^8 \text{ s}^{-1}$ ,  $3.7 \times 10^8 \text{ s}^{-1}$  and  $3.3 \times 10^8 \text{ s}^{-1}$  for tryptophan, porphyrin, and pyrene, respectively.

(a) For pyrene, the process will appear essentially as a pure dynamic quenching with reduced efficiency because  $m_1$  is large compared with  $m_0$ . Both intensity and lifetime

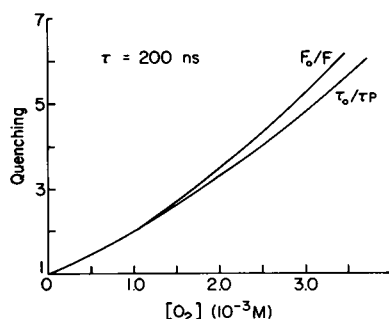


FIGURE 4 Quenching plots for a probe with  $\tau_0 = 200 \text{ ns}$ .  $F_0/F$ , quenching of intensity.  $\tau_0/\tau_P$ , quenching of lifetime. The lifetime is the apparent phase lifetime measured by phase fluorometry at 10 MHz modulation frequency. ( $k^+ = 5 \times 10^8 \text{ M}^{-1} \text{ s}^{-1}$ ,  $k^- = 2 \times 10^7 \text{ s}^{-1}$ ,  $\chi = 3 \times 10^8 \text{ s}^{-1}$ ).

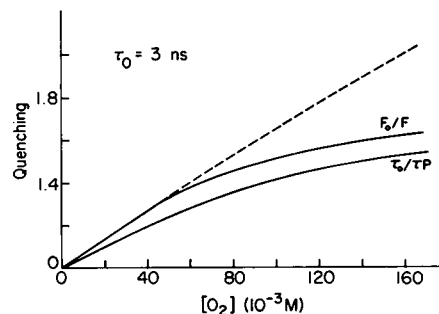


FIGURE 5 Quenching plots for a probe with  $\tau_0 = 3 \text{ ns}$ .  $F_0/F$ , quenching of intensity.  $\tau_0/\tau_P$ , quenching of lifetime as measured by phase fluorometry at 10 MHz modulation frequency. The dashed line was obtained using the high quencher concentration equations ( $k^+ = 5 \times 10^8 \text{ M}^{-1} \text{ s}^{-1}$ ,  $k^- = 2 \times 10^7 \text{ s}^{-1}$ ,  $\chi = 3 \times 10^8 \text{ s}^{-1}$ ,  $\chi' = 1.2 \times 10^9 \text{ s}^{-1}$ ).

quenching will behave similarly at low quencher concentration. A simulation of the quenching plots is reported in Fig. 4. High quenching is obtained at oxygen concentration as low as 3 mM. The simulation closely follows the results obtained by Vaughan and Weber (3). Note that a positive curvature in Stern-Volmer plots for both intensity and lifetime data in the case of proteins can result in the absence of the diffusion considerations such as those given in references 8–10.

(b) For tryptophan, because  $\Gamma$  is large, larger oxygen concentration is required for appreciable quenching. The molecules of protein contain one or more quenchers at the time of excitation and quenching proceeds as a dynamic process with diffusion inside the protein. Both fluorescence intensity and lifetime follow a similar behavior. A simulation of the quenching plots for the low concentration limit is reported in Fig. 5 (solid lines).

(c) For porphyrin, very appreciable quenching is observed when  $n \sim 1$ . Fluorescence intensity and lifetime will vary in a quite complex manner because of the simultaneous contributions to quenching from oxygen molecules that, at the time of excitation, are present both inside and outside the protein. In Fig. 6 we report the results of a simulation of the quenching plots for porphyrin.

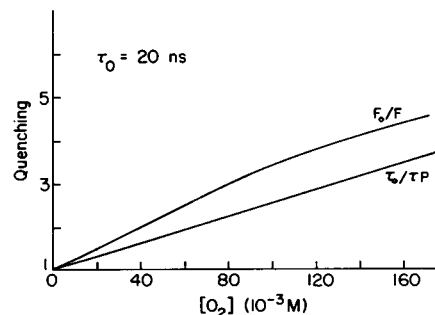


FIGURE 6 Quenching plots for a probe with  $\tau_0 = 20 \text{ ns}$ .  $F_0/F$ , quenching of intensity.  $\tau_0/\tau_P$ , quenching of lifetime as measured by phase fluorometry at 10 MHz modulation frequency ( $k^+ = 5 \times 10^8 \text{ s}^{-1} \text{ M}^{-1}$ ,  $k^- = 2 \times 10^7 \text{ s}^{-1}$ ,  $\chi = 3 \times 10^8 \text{ s}^{-1}$ ).

In Figs. 4–6, apparent values of the lifetime as measured by phase fluorometry at 10 MHz modulation frequency were used. In practice, a multiexponential decay should be observed and the apparent lifetime should be frequency dependent (see the companion paper).

In the high concentration limit Eqs. 17 and 18 must be used. As we already noted in the previous section, if  $\Gamma \ll \chi'$  then only the fluorescence intensity will be affected. This condition should be well verified for pyrene and porphyrin. For the tryptophan case we report in Fig. 5 a simulation of the expected quenching plot of the intensity for high concentration limit (dashed line). The quenching plots deviate from linearity (downward curvature) if the low concentration limit equations are used. If, instead, the complete equations are used, a much smaller curvature is observed.

In conclusion, the proposed model predicts characteristic differences in the intensity and fluorescence lifetime-quenching plots for probes with varying lifetimes in a protein interior. Furthermore a multiexponential decay must be easily recognizable for a probe with an unquenched lifetime around 20 ns. In the following paper, we show that the analysis proposed here applies to the oxygen quenching of the porphyrin fluorescence in  $\text{Hb}^{\text{des-Fe}}$  and  $\text{Mb}^{\text{des-Fe}}$ .

We would like to acknowledge the financial support of the National Science Foundation grant PCM 79-18646 and Biomedical Research Support grant PHS-2-507-RR07030-16 to Dr. Gratton, Institut National de la Santé et de la Recherche Médicale and Centre National de la Recherche Scientifique, France to Dr. Alpert and U. S. Public Health Service grant GM11223 to Dr. Weber.

Received for publication 25 July 1983 and in final form 29 November 1983.

## REFERENCES

1. Berlman, I. B. 1971. Handbook of Fluorescence Spectra of Aromatic Molecules. Academic Press, Inc., New York. 58–61.
2. Lakowicz, J. R., and G. Weber. 1973. Quenching of protein fluorescence by oxygen. Detection of structural fluctuations in proteins on the nanosecond time scale. *Biochemistry*. 12:4171–4179.
3. Vaughan, W. M., and G. Weber. 1970. Oxygen quenching of pyrenebutyric acid fluorescence in water. A dynamic probe of the microenvironment. *Biochemistry*. 9:466–473.
4. Weber, G. 1948. The quenching of fluorescence in liquids by complex formation. Determination of the mean lifetime of the complex. *Trans. Faraday Soc.* 44:185–189.
5. Weller, A. 1959. Outer and inner mechanism of reactions of excited molecules. *Discussions Faraday Soc.* 27:28–33.
6. Birks, J. B. 1970. Quenching of excited singlet and triplet states of aromatic hydrocarbons by oxygen and nitric oxide. *Proc. Int. Conf. Luminescence, Delaware*. F. Williams, editor. North-Holland Publishing Company, Amsterdam. 154–165.
7. Ware, W. R. 1962. Oxygen quenching in fluorescence in solution: an experimental study of the diffusion process. *J. Phys. Chem.* 66:455–458.
8. Nemzek, T. L., and W. R. Ware. 1975. Kinetics of diffusion-controlled reactions: transient effects in fluorescence quenching. *J. Chem. Phys.* 62:477–489.
9. Andre, J. C., M. Bouchy, and W. R. Ware. 1979. Kinetics of partly diffusion-controlled reactions. II. Theoretical treatment. *Chem. Phys.* 37:103–107.
10. Keizer, J. 1983. Nonlinear fluorescence quenching and the origin of positive curvature in Stern-Volmer plots. *J. Am. Chem. Soc.* 105:1494–1498.
11. Lakowicz, J. R., and G. Weber. 1973. Quenching of fluorescence by oxygen. A probe for structural fluctuations in macromolecules. *Biochemistry*. 12:4161–4171.
12. Coppey, M., D. M. Jameson, and B. Alpert. 1981. Oxygen diffusion through hemoglobin and  $\text{Hb}^{\text{desFe}}$ . *FEBS (Fed. Eur. Biochem. Soc.) Lett.* 126:191–194.